

## STEERING-CORRECTED 88 MHz QWRS FOR SARAF PHASE II\*

Jacob Rodnizki<sup>#</sup>, Joseph Ashkenazy, Dan Berkovits, Zvi Horvitz, Soreq NRC, Yavne, Israel  
Andrei Kolomiets, Brahim Mustapha, Peter Ostroumov, ANL, Argonne, IL 60439, U.S.A.

### Abstract

SARAF phase II linac is designed for 5 mA 40 MeV proton and deuteron beams. One of the design options is based on Quarter Wave Resonators (QWR). It is suggested to compensate the QWR non-symmetric magnetic field component by introducing a drift tube face tilt angle. Here we explore the applicability of this steering correction scheme to the acceleration of a CW high current low  $\beta$  light ion beam in an end-to-end 88 MHz QWR lattice. This can serve as a case study for multi-megawatt machines that are currently being designed by ANL. An analytical approximation is used to evaluate the on-axis beam steering behaviour. Two 88 MHz QWR cavities,  $\beta_g=0.08$  and  $0.15$ , were EM designed, field and beam dynamics were simulated and optimized. Using the tube face tilt angle concept the beam steering along a QWR can be reduced to the order of 0.1 mrad. Beam dynamics lattice examination including error analysis demonstrated an efficient high performance 40 MeV linac with 19 QWRs ( $E_p < 35$  MV/m,  $B_p < 70$  mT).

### QWR DESIGN AND FIELD SIMULATION

Two 88 MHz QWR cavities,  $\beta_g=0.08$  and  $0.15$ , were EM designed and the RF fields were simulated with CST MWS. Both cavity types were optimized for maximum efficient energy gain under the requirements of minimal  $B_p/E_{acc}$  and  $E_p/E_{acc}$ .  $B_p$  is typically located towards the upper part of the inner conductor, while  $E_p$  is typically located in the vicinity of the internal tube face, (Fig. 1). The fields obtained at recent ANL tests for a 73 MHz QWR,  $E_p=70$  MV/m and  $B_p=105$  mT, imply that, if state-of-the-art surface treatment is used,  $E_p$  is not a real limiting factor. The peak magnetic field, which then seems to be the primary barrier for the maximal reachable accelerating voltage, was minimized by tapering the inner and outer conductor walls [1]. The optimized values of  $B_p/E_{acc} = 0.74$  for the  $\beta_g=0.08$  cavity and  $B_p/E_{acc} = 0.80$  for the  $\beta_g=0.15$  cavity are lower than similar  $\beta_g$  state-of-the-art QWR and HWR cavities.

### ANALYTIC MODELING OF THE BEAM STEERING CORRECTION

The inherent asymmetry of QWR cavities results in the existence of on-axis transversal RF field components. The horizontal magnetic field,  $H_x$ , is the main cause of beam steering, while the vertical electric dipole field component,  $E_{yd}$ , may contribute significantly to the steering effect for  $\beta < \beta_g$ , values [2,3,4].  $H_x$ , as well as the accelerating field,  $E_z$ , are, to large extent, symmetric relative to the mid plane of each gap, where their maximal value is obtained, while their extension inside each tube scales with the tube diameter (Fig 2).

For low  $\beta$  SC QWR cavities the on-axis spatial field distributions can be approximated by  $H_x(z) = H_0e(z)$ , and  $E_z(z) = E_0e(z)$ , where:

$$e(z) = \begin{cases} \cos\left[\left(k_g z + \frac{\pi}{2}\right) \cdot \frac{1}{g}\right] & -\frac{\beta_g \lambda}{4} - \frac{d}{2} \leq z \leq -\frac{\beta_g \lambda}{4} + \frac{d}{2} \\ \cos\left[\left(k_g z - \frac{\pi}{2}\right) \cdot \frac{1}{g}\right] & \frac{\beta_g \lambda}{4} - \frac{d}{2} \leq z \leq \frac{\beta_g \lambda}{4} + \frac{d}{2} \\ 0 & \text{otherwise} \end{cases}$$

$k_g = 2\pi/\beta_g \lambda$ ,  $g = 2d/\beta_g \lambda$  and  $d = d_0 + 2\varepsilon$ , where  $d_0$  is the gap width and  $\varepsilon$  represents the extension of the field inside each tube. The vertical electric dipole field is reasonably approximated by a constant distribution over each (extended) gap [2].

A promising method for steering correction is the tilting of the tube faces by a small angle,  $\theta$ , [2]. Such a tilt results in an on-axis vertical electric field,  $E_{yt}$ , which, by applying Faraday's law, can be shown to be anti symmetric with regard to the mid plane of each gap, and to decay as  $\pm\theta E_z$  inside the internal/external tubes on the

Figure 1: 88MHz QWR  $\beta_g=0.08$  (top) &  $0.15$  CST (bottom) fields. For each cavity, the two left drawings show the electric field in vector and contour representations, while the two right drawings show the magnetic field.

\*Work supported by the U.S. Department of Energy, Office of Nuclear Physics, under Contract No. DE-AC02-06CH11357 and WFO 85Y47 supported by SNRC.

<sup>#</sup>jacob@soreq.gov.il

sides of the first gap and vice versa on the sides of the second gap. As such,  $E_{yt}$  has two extremal points in each gap and thus can be approximated by:

$$E_{yt}(z) = \frac{\theta}{\pi} E_0 \begin{cases} \sin \left[ \left( 2k_g z + \frac{\pi}{2} \right) \cdot \frac{1}{g} \right] & -\frac{\beta_g \lambda}{4} - \frac{d}{2} \leq z \leq -\frac{\beta_g \lambda}{4} + \frac{d}{2} \\ -\sin \left[ \left( 2k_g z - \frac{\pi}{2} \right) \cdot \frac{1}{g} \right] & \frac{\beta_g \lambda}{4} - \frac{d}{2} \leq z \leq \frac{\beta_g \lambda}{4} + \frac{d}{2} \\ 0 & \text{otherwise} \end{cases}$$

Calculating the contributions of the magnetic and electric fields to the steering angles ( $\alpha_h, \alpha_{yt}, \alpha_{yd}$ ) by integration over the on-axis particle passage while neglecting the particle axial acceleration [2, 4], and after some tedious manipulations, we obtain:

$$\alpha_h = -\frac{2ec\mu_0 H_0 \beta_g \lambda}{mc^2 \pi} \frac{g\beta}{g^2 \beta_g^2 - \beta^2} \cos\left(g \frac{\beta_g \pi}{\beta}\right) \sin\left(\frac{\beta_g \pi}{\beta}\right) \sin\varphi$$

$$\alpha_{yt} = \frac{eE_0 \theta}{mc^2 \pi} \frac{\beta_g \lambda}{\pi} \frac{4g}{g^2 \beta_g^2 - 4\beta^2} \sin\left(g \frac{\beta_g \pi}{\beta}\right) \sin\left(\frac{\beta_g \pi}{\beta}\right) \sin\varphi$$

$$\alpha_{yd} = -\frac{2eE_{yd} \lambda}{mc^2 \beta \pi} \sin\left(g \frac{\beta_g \pi}{\beta}\right) \cos\left(\frac{\beta_g \pi}{\beta}\right) \sin\varphi$$

where  $\varphi$  is the synchronous phase and  $m$  is the particle mass.

Fig. 2 shows CST simulated fields along the beam axis for  $\beta_g=0.08$  and  $\theta=2.5^\circ$ .  $E_y$  is the total vertical electric field consisting in fact of  $E_{yt}$  and  $E_{yd}$ . In order for all field components to appear on the same scale,  $E_y$  was divided by  $2\theta/\pi$  and  $H_x$  by  $-2\theta/(\pi\mu_0\beta_g c)$ .

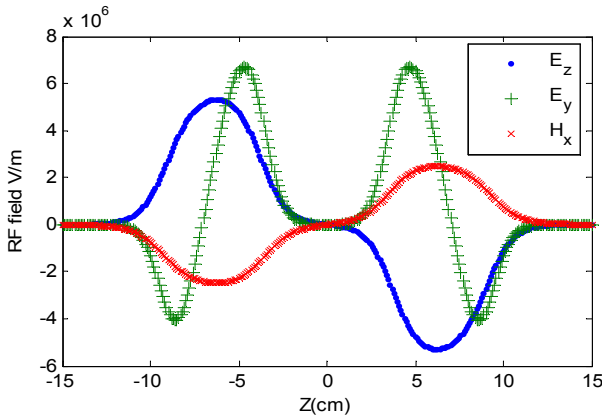


Figure 2: CST simulated fields along the beam axis for  $\beta_g=0.08$  and  $\theta=2.5^\circ$ .  $E_y$  was divided by  $2\theta/\pi$  and  $H_x$  by  $-2\theta/(\pi\mu_0\beta_g c)$ .

By fitting the above approximate analytical expressions for  $H_x$ ,  $E_{yt}$  and  $E_{yd}$  to the CST simulated on-axis fields we obtained the effective amplitudes ( $H_0$ ,  $E_0\theta/\pi$  and  $E_{yd}$ ), gap width ( $d$ ), and gap to gap distance (by modifying  $\beta_g$ ) for each of these field components. These fitted values were plugged in the expressions for  $\alpha_h$ ,  $\alpha_{yt}$  and  $\alpha_{yd}$ , which were evaluated as functions of  $\beta$  and  $\varphi$ . The evaluated steering

components along the QWR beam axis, including the sum of the electric field components  $\alpha_{yt} + \alpha_{yd}$ , and the total steering  $\alpha_{tot}$ , are shown in Fig 3 as functions of  $\beta$  for  $\beta_g=0.08$  and  $\varphi=-90^\circ$ . The field amplitudes (Fig. 2) correspond to a 1 Joule stored energy in the cavity. Shown also are the evaluations of the steering components at discrete  $\beta$  values calculated using the exact field distributions obtained with CST MWS. As can be seen, the derived steering model results fit very well to the steering values evaluated with CST MWS. Note that a good agreement is found also at  $\beta$  values much below  $\beta_g$ . This result, obtained with our approximation for the gap fields, has to be compared with the relatively low accuracy at  $\beta < \beta_g$ , obtained with the leading-order Fourier approximation [2] or with the square-wave approximation [3,4].

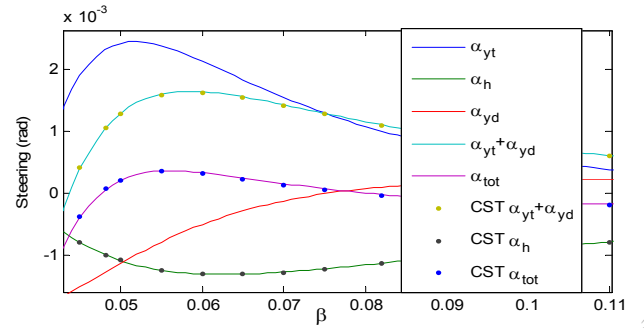


Figure 3: The  $\beta_g=0.08$  QWR electric and magnetic steering contributions as functions of  $\beta$  for a 1 Joule stored energy at  $\varphi=-90^\circ$ . The curves represent the results of the derived model while the dots were evaluated with CST MWS.

## OPTIMIZATION OF THE TILT ANGLE

The optimization of the drift tube face tilt angle is performed in two steps. In the first step, the tilt angle needed to compensate the magnetic steering at  $\beta_g$ ,  $\theta_g$ , is found as part of the cavity design phase with CST MWS described above. Since at  $\beta=\beta_g$ ,  $\alpha_{yd} \approx 0$  (see the analytic formula above), and since  $\alpha_{yt}$  is proportional to the tilt angle while  $\alpha_h$  is almost independent of it, we can write  $\theta_g = -\theta_0 \alpha_h / \alpha_{yt0}$ , where  $\theta_0$  is an initial guess for the tilt angle and  $\alpha_{yt0}$  is the resulting electric steering at  $\beta=\beta_g$ . In the second step the analytic model described above is used for a parametric study of  $\theta$  values around the  $\theta_g$  value obtained in the first step, until a value of  $\theta$  is found for which the total steering,  $\alpha_{tot}$ , is minimal over the desired  $\beta$  range. In the present study the derived tube face angles are  $2.5^\circ$  for the  $\beta_g=0.08$  QWR and  $8.3^\circ$  for the  $\beta_g=0.15$  QWR.

## BEAM DYNAMICS SIMULATIONS

An end-to-end 88 MHz beam dynamics lattice was designed and tested with the TRACK beam dynamics simulation code [5] for 40 MeV, 5 mA proton and deuteron beams. The lattice includes an RFQ, an MEBT with a buncher and four quadrupoles, and three cryostats

housing six superconducting solenoids, five  $\beta_g=0.08$  and fourteen  $\beta_g=0.15$  QWRs with steering correction. The design demonstrates an efficient acceleration with moderate fields for both proton and deuteron beams. A low transverse emittance growth and no longitudinal emittance growth was observed, for a proton beam (Fig. 4 bottom). For a nominal simulation, the beam centroid deviations from the axis, due to the residual steering along the QWRs, were below 0.7 mm for a 35 mm aperture diameter (Fig. 4 top). For a zero tilt angle, the beam centroid deviations were 5 times larger. Varying the beam aperture diameter in the 30-35 mm range did not affect significantly the QWR performance, while the larger aperture is expected to have lower beam losses.

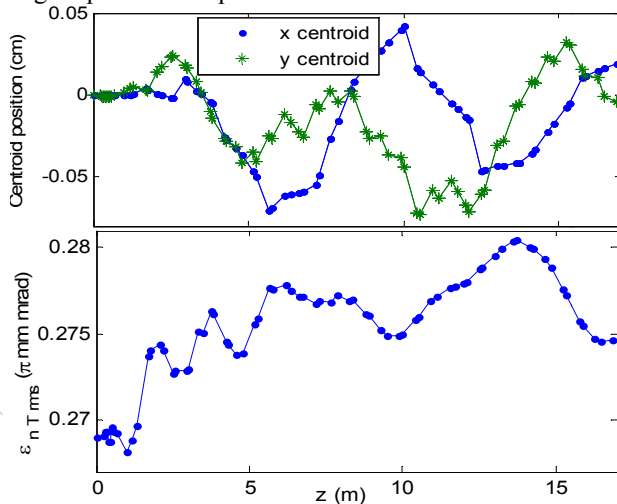


Figure 4: The beam centroid position along the linac (top) and the normalized transverse emittance growth along the linac (bottom) for a proton beam.

The deuteron energy gain in the QWRs along the linac as function of  $\beta$  is shown in Fig. 5 top. The lattice was examined for a loss of one  $\beta_g=0.08$  QWR at the downstream end of the low  $\beta$  section (Fig. 5 bottom). The resulted analysis demonstrated the lattice robustness. The energy gains of the QWRs  $\beta_g=0.15$  section were shifted by one towards the low  $\beta_g$  QWRs section and only the last QWR energy gain is missing. An error run for a feasible manufacture and operational error range with a 5 mA proton beam approve the linac could be operated CW while keeping the hands on maintenance criterion requirements (Fig. 6).

## SUMMARY

We have developed an analytical approach for calculating the QWR tube face angle in order to minimize the QWR steering effect. Proton and deuteron beam dynamics simulations show that a QWR steering corrected linac lattice is robust. However, since the resulted 0.15 QWR dimensions are large and challenging, a solution based on 0.15 QWR at 109 MHz, as in the ATLAS energy upgrade module, and 15 kW power supply is being studied for SARAF phase II.

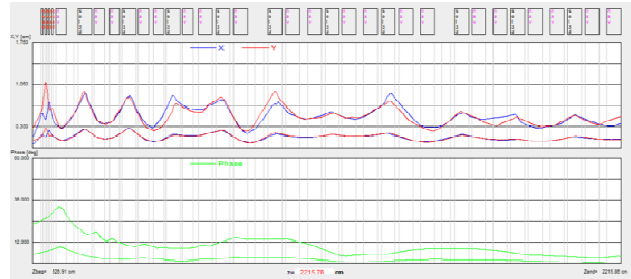
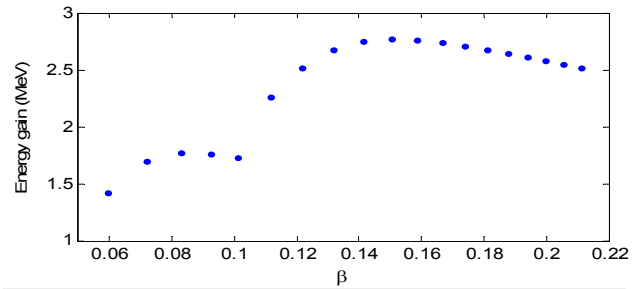


Figure 5: The QWRs energy gain along the linac for a 5 mA deuteron beam (top) and the beam dynamics lattice robustness for a loss of one  $\beta_g=0.08$  QWR (bottom).

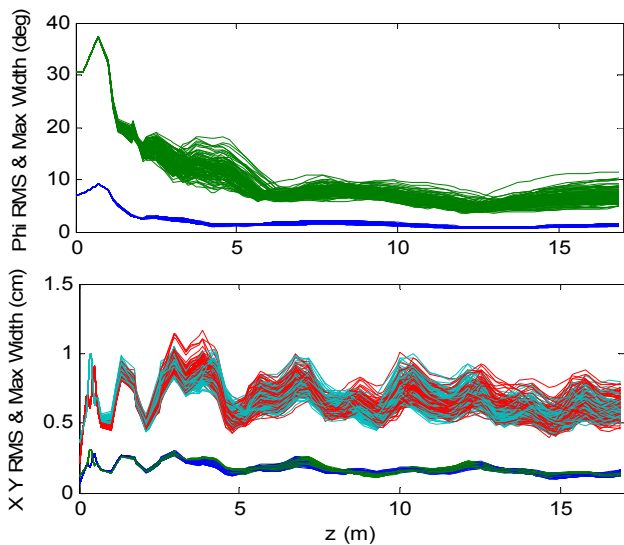


Figure 6: Error run study along the QWR linac, 100 error runs, 500k macro particles each.

## REFERENCES

- [1] B. Mustapha and P.N. Ostroumov, Electro-magnetic Optimization of a QWR, LINAC'10, Tsukuba (2010).
- [2] P. N. Ostroumov and K. W. Shepard, Correction of beam-steering effects in low-velocity SC quarter-wave cavities, PRST-AB, 4 110101 (2001).
- [3] M. A. Fraser, R. M. Jones and M. Pasini, BD design studies of a SC radioactive ion beam post accelerator, PRST-AB, 14, 020102 (2011).
- [4] A. Facco and V. Zvyagintsev, Beam steering in superconducting quarter-wave resonators: An analytical approach, PRST-AB, 14, 070101 (2011).
- [5] P. N. Ostroumov et al., Track Beam dynamics simulation code, TrackV37, (2007).